35th Annual International Conference of the IEEE EMBS
Osaka, Japan, 3 - 7 July, 2013

Physiological Control of Implantable Rotary Blood Pumps for Heart Failure Patients

Mohsen A. Bakouri, Robert F. Salamonsen, Andrey V. Savkin, Abdul-Hakeem H. Alomari, Einly Lim and Nigel H. Lovell.

Abstract— **In general, patient variability and diverse environmental operation makes physiological control of a left ventricular assist device (LVAD) a complex and complicated problem. In this work, we implement a Starling-like controller which adjusts mean pump flow using pump flow pulsatility as the feedback parameter. The linear relationship between mean pump flow and pump flow pulsatility forms the desired flow of the Starling-like controller. A tracking control algorithm based on sliding mode control (SMC) has been implemented. The controller regulates the estimated mean pulsatile flow $(\overline{Q}_p)$ and flow pulsatility (PI_{Q_p}) generated from a model of the assist device. A lumped parameter model of the cardiovascular system (CVS) was used to test the control strategy. The immediate response of the controller was evaluated by inducing a fall in left ventricle (LV) preload following a reduction in circulating blood volume. The simulation supports the speed and robustness of the proposed strategy.**

I. Introduction

In order to provide long-term alternative treatment for heart failure (HF) patients, design of physiological control for a left ventricular assist device (LVAD) is an important goal. This controller is required to improve the interaction between an implantable rotary blood pump (IRBP) and the cardiovascular system (CVS), and ideally restores the Frank-Starling mechanism of the heart. This ensures that the output of the left ventricle (LV) is adjusted to compensate for changes in LV end-diastolic pressure such that it ejects whatever blood it receives from the pulmonary circulation [1]. Different physiological control strategies have been proposed for IRBPs by various groups in recent years [2]–[5]. However, none have achieved widespread acceptance by the medical profession [6]. Recently, our research group has developed and validated numerically an approach that uses pulsatility measures derived for IRBPs to be used as surrogates for LV stroke work, which relates more directly to pulsatility than LV preload. This strategy enables the development of a Starling-like controller which affords true physiological control of the LVAD [7]. Previously, Choi et al. [8] used pump flow pulsatility as sensor-less surrogate for LV filling pressure and to give more physiological information that may be helpful to the clinician. It is clearly known that pump flow is pulsatile over each cardiac cycle and its magnitude is proportional to the force of left ventricular contraction (stroke work of the heart). We refer to this as flow pulsatility. Because of this we have to control the average flow of the pump rather than instantaneous flow.

The aim of the present work is to regulate the flow error to a set point without inducing suction in the ventricle. The controller is designed to minimize the error between the desired and estimated mean pump flow. A robust sliding mode control (SMC) is specifically used in this study because it is particularly suited for systems that are complex and show parameter uncertainties. Different system states were optimally estimated using a linear quadratic estimator (LQE) due to the presence of disturbance and measurement noise. In this study, the feasibility of implementing a Starling-like controller based on pump flow pulsatility was studied using a computer simulation. A non-invasive state space model estimator of the LVAD was used to construct this controller [9].

II. Materials and Methods

A. Control strategy

Salamonsen et al. [7] have assumed that while the aortic valve is closed, total cardiac output can be approximated as pump flow. This leads to a linear relationship between mean pump flow and flow pulsatility which forms the target flow for a Starling-like controller. This paper proposes a method to utilize this approach to specify the set-point for pump flow using non-invasive measurements. Fig. 1 illustrates the immediate response of a proposed Starling-like controller. When a change in system state from S1 to S2 or S3 causes a deviation in the operating point from the intersection of S1 and CLn (○) to (◎) on S2 or S3, the controller responds by returning the operating points along a radial path with center of rotation at origin of axes, to the control line CLn, settling to positions (●) at the intersection of CLn and state lines S2 or S3. The following equation is used to control this operation.

$$\overline{Q}_{pr,t} = \left(\sqrt{(\overline{Q}_{p,t-1})^2 + (PI_{Qp,t-1})^2}\right) \cdot \sin\theta_n \qquad (1)$$

M. A. Bakouri and A. V. Savkin are with the School of Electrical Engineering and Telecommunication, The University of New South Wales, Sydney, NSW 2052, Australia (phone: +61 (2) 9385 6359. e-mail: m.bakouri@student.unsw.edu.au; e-mail: a.savkin@unsw.edu.au)

R. F. Salamosen is with Intensive Care, Alfred Hospital, Melbourne, Victoria, Australia, and also with Department Epidemiology and Preventive Medicine, Monash University, Melbourne, Victoria 3800, Australia e-mail: rsalamon@iinet.net.au.

A. H. Alomari is with Department of Biomedical Engineering, University of Dammam, Dammam (31451) Saudi Arabia e-mail: ahalomari@ud.edu.sa.

E. Lim is with Department of Biomedical Engineering, The University of Malaya, Kuala Lumpur, Malaysia e-mail: einlylim@um.edu.my.

N. H. Lovell is with the Graduate School of Biomedical Engineering, The University of New South Wales, Sydney, NSW 2052, Australia e-mail: n.lovell@unsw.edu.au.

978-1-4577-0216-7/13/$26.00 ©2013 IEEE

where, $\overline{Q}_{pr,t}$ is desired pump flow, $\overline{Q}_p$ is estimated mean pump flow, PI_{Q_p} is pulsatility of pump flow and θ_n is the angle of gradient. The upper and lower limits for both mean pump flow and pump flow pulsatility are implemented to modify the control gradient. Fig. 2 illustrates the block diagram of the proposed control strategy.

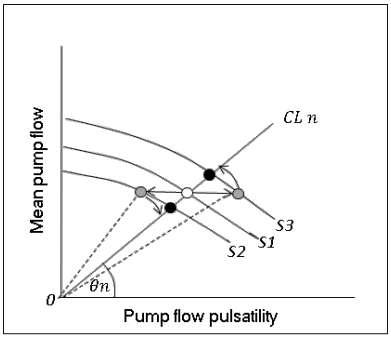

Fig. 1. Immediate response of the Starling-like pump flow controller to change in system states.

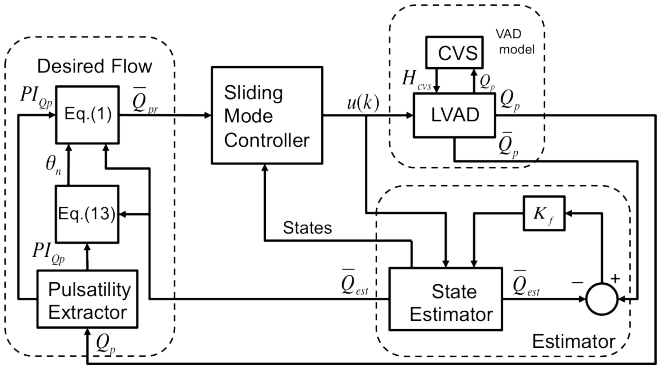

Fig. 2. Block diagram of control system.

B. Controller design

The model of LVAD is identified by an ARX model [9], as:

$$\begin{aligned} x(k+1) &= Ax(k) + \delta Ax(k) + Bu(k) + \zeta(k) \\ y(k) &= Cx(k) \end{aligned} \tag{2}$$

where $x \in R^n$ is the system states, $u \in R^m$ is the control input, δA is the system parameter variation, $\zeta(k)$ is the system disturbance, $y \in R^r$ is the system output, A, B and C are compatibly dimensioned matrices.

The controller was designed using SMC based on pole placement technique that has introduced by Edward and Spurgeon [10]. In this technique, the control system matrix is known as $(A - BK)$ [11]. Where $K \in R^n$ is a gain matrix obtained by assigning n desired eigenvalues in pole placement.

In this strategy, the Gao reaching law has chosen to implement the control algorithm [12]. This reaching law is defined as:

$$s(k+1) = (1 - qT)s(k) - \epsilon T \text{sign}(s(k)) \tag{3}$$

where, $T > 0$ is the sampling period, $\epsilon > 0$ $q \geq 0$ such that $0 < (1 - qT) < 1$.

We define the sliding surface as:

$$s(k) = \mu x(k) \tag{4}$$

where μ is a constant vector, designed based on the method that described in [13] to ensure that $x(k)$ is asymptotically stable. To satisfy the reaching law in Eq. 3, we obtain:

$$s(k+1) = \mu x(k+1) \tag{5}$$

From Eq. 2 and Eq. 4, we get:

$$\begin{aligned} &s(k+1) = \mu x(k+1) = \\ &\quad \mu(A - BK)x(k) + \mu\delta Ax(k) + \mu Bu(k) + \mu\zeta(k) \end{aligned} \tag{6}$$

The equalization of Eq. 3 and Eq. 6 gives:

$$\begin{aligned} &\mu(A - BK)x(k) + \mu\delta Ax(k) + \mu Bu(k) + \mu\zeta(k) = \\ &\quad (1 - qT)s(k) - \epsilon T \text{sign}(s(k)) \end{aligned} \tag{7}$$

From the Eq. 7, the control input signal $u(k)$ is:

$$\begin{aligned} u(k) = -(\mu B)^{-1}(&\mu(A - BK)x(k) + \mu\delta Ax(k) + \mu\zeta(k) \\ &+ (qT - 1)\mu x(k) + \epsilon T \text{sign}(s(k))) \end{aligned} \tag{8}$$

As δA and $\zeta(k)$ are unknown, the control law cannot be implemented unless we assume that the upper and lower bounded of the value $(\mu\delta Ax(k)) + \mu\zeta(k)$ are known as:

$$-D < (\mu\delta Ax(k)) + \mu\zeta(k) < D \tag{9}$$

then the control law can be re-written as:

$$\begin{aligned} u(k) = -(\mu B)^{-1}(&\mu(A - BK)x(k) + D\text{sign}(s(k)) \\ &+ (qT - 1)\mu x(k) + \epsilon T \text{sign}(s(k))) \end{aligned} \tag{10}$$

In this design, LQE has been introduced as in [14] to find an optimal state estimation by minimizing the following cost function:

$$min_u \int_0^\infty (x^T Qx + u^T Ru)dt \tag{11}$$

The solution to the optimization problem is the optimal Kalman gain (K_f).

where

$$K_f = PC^T R^{-1} \tag{12}$$

and P is known as the algebraic Riccati equation's solution.

The reference pump flow $\overline{Q}_{pr}$ was calculated using the gradient angle (θ) of the control line as:

$$\theta = K_{p,\theta}(e_{\overline{Q_p}} + e_{PI(Q_p)}) + K_{i,\theta} \int (e_{\overline{Q_p}} + e_{PI(Q_p)}) \quad (13)$$

where K_p and K_i are the proportional and integral gains. The gradient angle θ is automatically adjusted to insure that $\overline{Q}_p$ and PI_{Q_p} remain within their corresponding upper or lower limits for each cycle of the model using a proportional integral controller. So, the reference pump flow can be given as stated in Eq. 1. The merits of the designed algorithm were verified by numerical simulation using Matlab-Simulink (The Math-Works Inc., Natick, MA, USA).

C. Simulation protocols

The control strategy was assessed using a software model incorporating a lumped-parameter model of CVS in combination with a stable dynamic model of an LVAD [15]. The design parameters of the sliding surface in Eq. (10) is $\mu = [0.9413 \quad -0.0805]$ and those of the control law in the same equation are $qT = 0.01$ and $\epsilon T = 0.02$.

In this strategy, the total circulatory volume (V_{total}) was linearly decreased, in order to assess the immediate response of the controller to short-term circulatory changes. At 25 seconds, V_{total} decreased by 500 mL, and the simulation was continued for another 35 seconds to allow the system to reach a steady state corresponding to the new parameters values. In the simulations, the lower and upper limits for pump flow pulsatility were set to 1.5 and 4 L/min, while lower and upper limits for mean pump flow were set to 3 and 6 L/min.

III. Results and Discussion

Fig. 3 illustrates the immediate response of the controller to a reduction in V_{total}. The reduction in V_{total} produced a shift to the left of both LV and right ventricle (RV) pressure-volume loops, causing a reduction in end-diastolic and end-systolic volumes and pressures in both ventricles. The controller responds to a decrease in the LV preload and subsequently pump flow pulsatility by decreasing mean pump speed from 1350 rpm to 955 rpm and mean pump flow from 5.2 L/min to 2.8 L/min. Fig. 4 shows the estimated mean pulsatile flow in comparison with actual mean pump flow during the transient response of the simulation. Linear regression analysis between estimated and actual flow was implemented using MATLAB simulink. Fig. 5 illustrates the estimated steady state pump flow corresponding to a range of actual pump flows. Correlation between actual and estimated was highly significant ($R^2 = 0.9999$), and the slope was unity for the linear regression.

From the results, an inherent problem was observed. Not shown in this simulation is the occurrence of suction if the controller does not decrease pump flow quickly enough. Furthermore, the controller possesses a facility to increase or decrease the gain of the controller if very marked changes in cardiovascular state render the current controller settings inappropriate. This facility incorporating a dead zone combined with a PID controller was designed to control the angle of gradient to prevent dangerous states like over pumping and consequent ventricular suction. Also, it was noticed that the

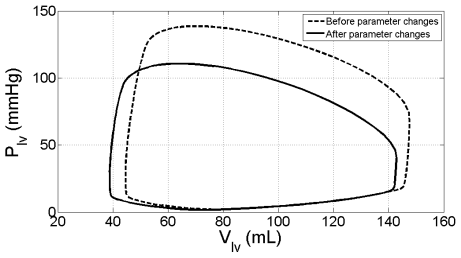

(a) LV volume versus LV pressure.

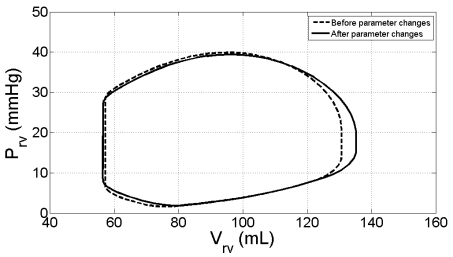

(b) RV volume versus RV pressure.

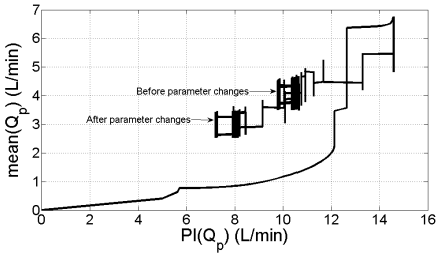

(c) Pump flow pulsatility versus mean pump flow.

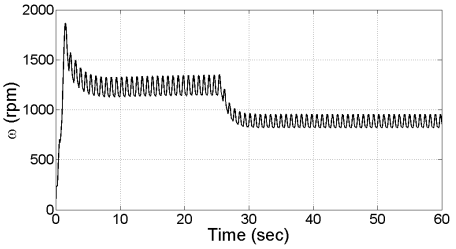

(d) Pump rotational speed.

Fig. 3. The immediate response of the controller to a reduction of total circulatory volume (V_{total}).

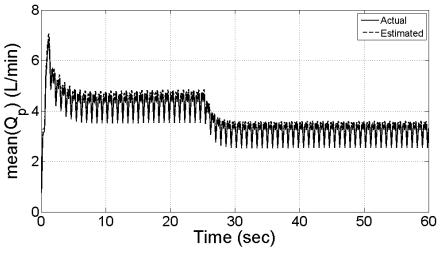

Fig. 4. Estimated mean pulsatile flow in comparison with actual mean pump flow at V_{total} scenario.

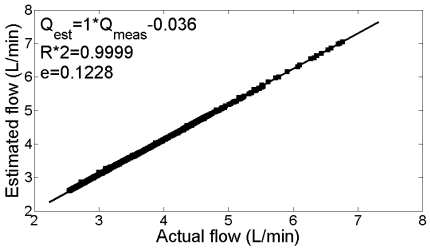

Fig. 5. Estimated steady state pump flow versus actual steady state pump flow at V_{total} scenario.

SMC is a very effective theory to deal with the errors in estimation of flow pulsatility.

Although space restrictions allow simulation of controller response to only one condition, there are a host of body conditions (causing migration of the operating point to S2 or S3 in Fig. 1) which call for less or more output from the heart. These include exercise, posture, anxiety states, sleep/wake cycles, and changes in medical treatment. We have successfully simulated changes in afterload and exercise with controller performance almost identical to the blood loss scenario studied here. One interesting change in state is the occurrence of aortic valve incompetence. While this reduces the efficacy of pump flow it also increases flow pulsatility, thus correcting the problem to some degree.

One limitation of the present study is that the designing controller was based on the pulsatility method. This method needs the natural heart to retain some residual contractility to provide pump flow pulsatility. Thus, this strategy would not be beneficial if the heart is not able to provide some output. There are some strategies that have tried to alleviate this concern. For example, Choi at al. [4] used the pulsatility ratio of the pump flow and pressure difference across the pump as a reference control index so that, the controller successfully adjusts the pump speed and supports the natural heart under different operation condition. In addition, Arndt et al. [3] developed a new control algorithm based on the pulsatility gradient with respect to rotational speed. This strategy enables the pump to operate at two distinct operating points that can be selected by physician according to the indicated therapeutic goal. In addition, Fig. 4 indicates the transient overshoot to 7 l/min at the beginning of the simulation before a steady state is achieved. Further tuning of the controller is required to eliminate this problem; see e.g. [16], [17].

Even though we have successfully evaluated this control strategy using a parameter optimized model of the cardiovascular system and rotary blood pump we regard this paper as the first stage only and plan to continue with studies in the mock loop and animal model in the near future.

IV. Conclusion

In this paper, a physiological controller which mimics the Frank-Starling law of the heart has been developed. The controller adjusts mean pulsatile flow using pump flow pulsatility as the feedback parameter. A novel robust SMC technique is proposed. The control strategy was evaluated using a lumped parameter model of the CVS. Immediate response of the controller to changes in V_{total} was assessed. Simulation results demonstrate that the control algorithm was able to drive the system states with stable and brief transients in changes in the response to CVS.

Acknowledgment

This work was supported in part by the Australian Research Council. E. Lim thanks the Ministry of Higher Education (MOHE) of Malaysia (UM.C/HIR/MOHE/ENG/50) for providing the research grant support.

References

[1] A. C. Guyton and J. Hall, *Textbook of medical physiology*. Elsevier Saunders, 2006.

[2] E. Lim, A. H. Alomari, A. V. Savkin, S. Dokos, J. F. Fraser, D. L. Timms, D. G. Mason, and N. H. Lovell, "A method for control of an implantable rotary blood pump for heart failure patients using noninvasive measurements," *Artificial Organs*, vol. 35, no. 8, pp. E174–E180, 2011.

[3] A. Arndt, P. Nüsser, K. Graichen, J. Müller, and B. Lampe, "Physiological control of a rotary blood pump with selectable therapeutic options: control of pulsatility gradient," *Artificial Organs*, vol. 32, no. 10, pp. 761–771, 2008.

[4] S. Choi, J. R. Boston, and J. F. Antaki, "Hemodynamic controller for left ventricular assist device based on pulsatility ratio," *Artificial Organs*, vol. 31, no. 2, pp. 114–125, 2007.

[5] Y. Wu, "Adaptive physiological speed/flow control of rotary blood pumps in permanent implantation using intrinsic pump parameters," *ASAIO Journal*, vol. 55, no. 4, pp. 335–339, 2009.

[6] A. H. AlOmari, A. V. Savkin, M. Stevens, D. G. Mason, D. L. Timms, R. F. Salamonsen, and N. H. Lovell, "Developments in control systems for rotary left ventricular assist devices for heart failure patients: a review," *Physiological measurement*, vol. 34, no. 1, pp. R1–R27, 2013.

[7] R. F. Salamonsen, E. Lim, N. Gaddum, A.-H. H. AlOmari, S. D. Gregory, M. Stevens, D. G. Mason, J. F. Fraser, D. Timms, M. K. Karunanithi *et al.*, "Theoretical foundations of a starling-like controller for rotary blood pumps," *Artificial Organs*, vol. 36, no. 9, pp. 787–796, 2012.

[8] S. Choi, J. Antaki, R. Boston, and D. Thomas, "A sensorless approach to control of a turbodynamic left ventricular assist system," *IEEE Transaction on Control System Technology*, vol. 9, no. 3, pp. 473–482, 2001.

[9] A.-H. AlOmari, F. Javed, A. V. Savkin, E. Lim, R. F. Salamonsen, D. G. Mason, and N. H. Lovell, "Non-invasive measurements based model predictive control of pulsatile flow in an implantable rotary blood pump for heart failure patients," in *Proceeding of the 19th Mediterranean Conference on Control & Automation*. IEEE, 2011, pp. 491–496.

[10] C. Edwards and S. Spurgeon, *Sliding mode control: theory and applications*. CRC Press, 1998, vol. 7.

[11] Y. Chung, B. Wen, and Y. Lin, "Optimal fuzzy sliding-mode control for bio-microfluidic manipulation," *Control Engineering Practice*, vol. 15, no. 9, pp. 1093–1105, 2007.

[12] W. Gao, Y. Wang, and A. Homaifa, "Discrete-time variable structure control systems," *IEEE Transactions on Industrial Electronics*, vol. 42, no. 2, pp. 117–122, 1995.

[13] S. K. Spurgeon, "Hyperplane design techniques for discrete-time variable structure control systems," *International Journal of Control*, vol. 55, no. 2, pp. 445–456, 1992.

[14] G. C. Goodwin, S. F. Graebe, and M. E. Salgado, *Control System Design*. Prentice Hall New Jersey, 2001, vol. 240.

[15] E. Lim, S. Dokos, S. L. Cloherty, R. F. Salamonsen, D. G. Mason, J. A. Reizes, and N. H. Lovell, "Parameter-optimized model of cardiovascular–rotary blood pump interactions," *IEEE Transactions on Biomedical Engineering*, vol. 57, no. 2, pp. 254–266, 2010.

[16] A. V. Savkin and I. R. Petersen, "Robust h^∞ control of uncertain linear systems with structured uncertainty," *Mathematical Systems, Estimation and Control*, vol. 6, no. 3, pp. 339–342, 1996.

[17] A. V. Savkin, I. R. Petersen, E. Skafidas, and R. J. Evans, "Hybrid dynamical systems: robust control synthesis problems," *Systems & control letters*, vol. 29, no. 2, pp. 81–90, 1996.